Global analysis of chromosome X gene expression in primary cultures of normal ovarian surface epithelial cells and epithelial ovarian cancer cell lines

MARIE-HÉLÈNE BENOÎT[1], THOMAS J. HUDSON[1,2,3], GEORGES MAIRE[4], JEREMY A. SQUIRE[4,5], SUZANNA L. ARCAND[6], DIANE PROVENCHER[7,8], ANNE-MARIE-MES-MASSON[7,9] and PATRICIA N. TONIN[1,3,6]

[1]Department of Human Genetics, McGill University, Montreal, Quebec H3A 1A1; [2]McGill University and Genome Quebec Innovation Centre, Montreal, Quebec H3A 1A4; [3]Department of Medicine, McGill University, Montreal, Quebec H3G 1A4; [4]Applied Molecular Oncology, The Ontario Cancer Institute, Princess Margaret Hospital, Toronto, Ontario M5G 2M9; [5]Departments of Medical Biophysics and Laboratory of Medicine and Pathobiology, University of Toronto, Toronto, Ontario M5G 1L5; [6]The Research Institute of McGill University Health Center, Montreal, Quebec H3G 1A4; [7]Centre de Recherche du Centre Hospitalier de l'Université de Montreal (CR-CHUM)/Institut du cancer de Montréal, Montreal, Quebec H2L 4M1; [8]Division de gynécologie et obstétrique, and [9]Départément de médicine, Université de Montréal, Montreal, Quebec H3C 3J7, Canada

Received June 2, 2006; Accepted August 3, 2006

Abstract. The interpretation of loss of heterozygosity (LOH) in cancers is complicated as genes that map to LOH regions may be transcriptionally active (Xa) or inactive (Xi) due to X chromosome inactivation (XCI). We have analyzed the chromosome X transcriptome in four epithelial ovarian cancer (EOC) cell lines (TOV21G, TOV81D, TOV112D, and OV90) and 12 primary cultures of normal ovarian surface epithelial (NOSE) cells in relation to chromosome X integrity. Two-way comparative analysis using HuGeneFL Affymetrix GeneChips® of TOV21G, TOV81D and OV90 relative to the NOSE samples was highly correlated (>89%) in contrast to that of TOV112D (56-69%). TOV112D, followed by TOV21G, exhibited the largest number of up-regulated genes. *XIST* expression by RT-PCR was not detectable in TOV112D or TOV21G. Allele-specific transcription by cDNA sequence analysis of genes known to be subjected to XCI revealed maintenance of XCI in TOV81D and OV90, but not TOV21G. Biallelic expression could not be assessed in TOV112D due to reduction to hemizygosity of chromosome X. Chromosome X rearrangements were observed in FISH analysis of TOV112D and TOV21G, and both of these EOC cell lines were negative for Barr body analysis. The differentially expressed genes did not appear to map to any particular region of the X chromosome in any EOC cell line. The absence of *XIST* expression is consistent with Barr body loss in TOV112D and TOV21G. The combined evidence is consistent with two proposed mechanisms to account for absence of Xi in female cancers: Xi loss followed by Xa duplication (exemplified by TOV112D) and transcriptional reactivation of Xi (exemplified by TOV21G). Despite an alteration in *XIST* expression and differences in allelic content in the EOC cell lines, the chromosome X transcriptome was modified modestly when compared with that of NOSE samples.

Correspondence to: Dr Patricia N. Tonin, Medical Genetics, Montreal General Hospital, Room L10-120, Montreal, Quebec H3G 1A4, Canada
E-mail: patricia.tonin@mcgill.ca

Key words: chromosome X, ovarian cancer

Introduction

Cytogenetic and molecular genetic mapping studies of ovarian carcinomas have identified consistent structural and numerical anomalies involving chromosome X. Loss of heterozygosity (LOH) analyses have identified minimal regions of overlapping deletions of Xp22.2-22.3, Xp21.1-p11.4, Xp11.2, Xq11.2-q12, Xq21-q23, and Xq25-q26 (1-8). The biological significance of these events is unknown. However, LOH of the Xq25-q26.1 region has been correlated with high-grade carcinomas (6), and loss of the Xp22.2-q21 region has been associated with the development of cisplatin resistance (9). LOH of Xq11-q12 has been shown to be associated with a greater risk of ovarian cancer progression, and LOH of Xq21-q23 was proposed as an independent prognostic factor of survival. Comparative genomic hybridization studies have also suggested losses and as well as gains of chromosome X loci (10-14). These findings suggest that the regions exhibiting LOH harbor tumor suppressor genes (TSG) important in ovarian cancer. However, interpreting the significance of LOH studies is complicated because allelic imbalances can involve chromosomal regions that are subjected to X chromosome inactivation (XCI), and thus associated with either transcriptionally active (Xa) or inactive (Xi) genes (15,16). For example, the LOH of Xp22.2-22.3 observed in ovarian tumors preferentially involves loss of the Xa allele (1). Monoallelically expressed oncogenes can

become overexpressed following gains of Xa, irrespective of increases in the copy number of chromosome X. While LOH of the Xi allele might have little or no impact, LOH of the Xa allele alone would be sufficient to silence a TSG that is subjected to XCI (17,18). In addition, perturbations of XCI mechanisms associated with the transcriptional reactivation of genes that are normally silenced on Xi could result in altered gene expression. Thus conventional LOH analysis of chromosome X poses an interesting challenge in establishing both the importance of chromosome X anomalies in ovarian cancer and the elucidation of TSGs important in this disease.

Microarray analysis of gene expression affords the opportunity to assess the expression of a large number of genes simultaneously. Recently we have applied Affymetrix GeneChip® arrays to assess expression patterns in four spontaneously immortalized epithelial ovarian cancer (EOC) cell lines derived from malignant ovarian tumors (TOV21G, TOV81D, and TOV112D) and ascites (OV90) in comparison to primary cultures of normal ovarian surface epithelial (NOSE) cells (19-23). These EOC cell lines have been studied extensively for their growth characteristics in *in vivo* and *in vitro* models of ovarian tumorigenesis and they have been shown to represent the clinical behavior of the ovarian cancers from which they were derived (24). Most notably, the cell line TOV81D, which does not form tumors in mouse models of tumorigenesis, was derived from a patient that exhibited the most indolent form of ovarian malignant disease (24). The phenotype of the EOC cell lines was also reflected by microarray expression profiles for overall global gene expression (19) and for the expression of genes on specific chromosomes, such as chromosomes 3, 17, and 22 (20-22). In the present study we have assessed the expression of chromosome X genes in the four EOC cell lines and compared their expression profiles with a series of 12 primary cultures of NOSE samples. The clonal nature of EOC (25-29) facilitates the interpretation of differentially expressed genes with regards to XCI status as it is anticipated that genes subjected to XCI will be expressed exclusively from the same parental allele in the EOC cell lines. We have also related chromosome X gene expression with the cytogenetic, genomic heterozygosity and Barr body status of EOC cell lines.

Materials and methods

Primary cultures of NOSE and EOC cell lines, and ovarian tumor samples. Primary cultures were derived from NOSE cells from ovaries of 12 participants and established as described elsewhere (21,30,31). The NOSE samples were derived from the ovaries of women with no prior history of ovarian cancer following prophylactic oophorectomy at the CHUM's Hôpital Notre-Dame. The EOC cell lines were established from ovarian malignant tumors (TOV81D, TOV21G and TOV112D) and from ovarian malignant ascites (OV90) of chemotherapy naïve patients as described (24). They were derived from a grade 1-2 and stage IIIc papillary serous adenocarcinoma (TOV81D), a grade 3 and stage III clear cell carcinoma (TOV21G), a grade 3 and stage IIIc endometrioid carcinoma (TOV112D), and from the ascites fluid of a grade 3 and stage IIIc adenocarcinoma (OV90). Cells were cultured in OSE medium consisting of 50:50 medium 199:105 (Sigma, Oakville, Ontario), 2.5 μg/ml amphotericin B and 50 μg/ml gentamicin. Culture media were supplemented with 15% fetal bovine serum for the NOSE cultures and 10% fetal bovine serum for the EOC cell lines.

Ovarian tumor tissues (TOV921G, TOV1118D, TOV837, TOV1054G, TOV1108D, TOV1010G, TOV908D, TOV800EP, TOV1142D, TOV750, TOV1095D, TOV863D, TOV1148G, TOV947EP, and TOV1147D) were obtained following surgery from the CHUM-Hôpital Notre-Dame as described (32). Histopathology was determined in accordance with criteria established by the International Federation of Gynecologists and Oncologists (FIGO). All samples were from chemotherapy naïve patients.

Nucleic acid extraction. DNA was extracted from EOC cell lines as described previously (31). Total RNA was extracted with TRIzol™ reagent (Gibco/BRL, Life Technologies Inc., Grand Island, NY) from the primary cultures of NOSE samples and EOC cell lines grown to 80% confluence in 100-mm petri dishes and frozen tumors samples as described (21). The quality of the RNA for expression microarray analysis was assessed by gel electrophoresis and by the 2100 Bioanalyzer using the RNA 6000 Nano LabChip kit (Agilent Technologies, Germany).

Microarray analysis. Expression analysis was performed using the Affymetrix GeneChip® HuGeneFL and HG-133A arrays (Santa Clara, CA) (affymetrix.com). The HuGeneFL array was used to assess the expression analysis of 12 NOSE samples (NOV31, NOV61, NOV116D, NOV220D, NOV319, NOV436G, NOV504D, NOV653G, NOV821, NOV848D, NOV900, and NOV910G) and EOC cell lines (TOV81D, OV90, TOV21G and TOV112D). The HG-133A array was used to assess the expression of a smaller series of NOSE samples (NOV31, NOV61, and NOV653G) and the EOC cell lines. Microarray experiments were performed once per sample tested. Hybridization and scanning were performed at the McGill University and Genome Quebec Innovation Centre (genomequebec.mcgill.ca). Total RNA was used to prepare a biotinylated hybridization target and hybridization was performed as described (genomequebec.mcgill.ca).

Gene expression levels were determined from scanned images of HuGeneFL and HG-133A arrays using MAS4 and MAS5 software (Affymetrix® Microarray Suite), respectively. The software generates an average difference ratio (or raw expression value) across the 13-20 probe pairs that correspond to a sequence matched probe set, as well as a reliability score indicating the variability of hybridization signal within each probe set which reflects hybridization to a probe set containing a single nucleotide mismatch: Present (P), Marginal (M), or Ambiguous (A). The P call reflects the highest reliability score, and represents a minimal hybridization to the mismatch probe set and consistent hybridization across all matched probes. Data with low reliability scores (A calls) across all samples tested for a given probe set were removed from further analysis, as these expression values may reflect either low expression values or indistinguishable hybridization of matched and mismatched probe sets. In order to eliminate systematic biases when comparing the expression values from independently generated data sets, the raw data was re-scaled (normalized)

by multiplying the value for individual probe sets by 100 and dividing by the mean of the raw expression values for the given data set, as described (21-33).

Extractor© v.4 (Lypny and Tonin 2002), a data filtering software application written using an xTalk scripting language (MetaCard Corporation) was used to retrieve probe sets representing known or hypothetical genes that map to chromosome X according to the UniGene database July 2004 version (ncbi.nlm.nih.gov). Using the most recent assembly, 215 and 766 probe sets were identified that were associated with chromosome X genes from the HuGeneFL and HG-133A arrays, respectively. Probe sets were aligned to chromosome X using the accession numbers corresponding to the representative gene and the base pair position according to the UCSC Genome Browser (May 2004, hg 17 Assembly; genome.ucsc.edu/goldenPath/hgTracks.html). Additional information for the genes represented by the probe sets was obtained from the NetAffx™ Analysis Center (Affymetrix.com).

Hierarchical clustering (Pearson's correlation) of normalized expression values was performed using GeneSpring™ software (Silicon Genetics). Correlation analysis was performed with Microsoft® Excel. Statistical analyses of differentially expressed probe sets in comparative analyses of chromosome Xp and Xq arm genes were performed using two-side Fisher Exact test (http://home.clara.net/sisa/).

In order not to overestimate gene expression differences resulting from the higher variability of low values of expression, a threshold value of 20 or 15 was assigned to probe sets whose expression values fell in the lower range of expression for the HuGeneFL and HG-133A array data sets, respectively. The threshold value used for re-scaling is based on the mean of expression values, for the given GeneChip, of probe sets with low reliability scores (A calls). Two-way comparative analyses were performed based on comparison of re-scaled data of each EOC cell line and the maximum or minimum value of expression of the NOSE samples. Expression values of the chromosome X derived data and two-way comparative analyses of re-scaled data are available in supplementary tables (www.toninlab.mcgill.ca).

RT-PCR analysis of XIST. Reverse transcriptase-PCR analysis was performed with cDNA prepared from total RNA using SuperscriptII reverse transcript enzyme as described (23). The primer sequences used for RT-PCR analysis of *XIST* were 5'CTTGAAGACCTGGGGAAATCCC3' (forward) and 5'TGTCAATCTAAAGGTAACCGGC3' (reverse) (34). PCR reactions for the test gene were performed in parallel with an internal reference primer designed to amplify *18S* RNA essentially as described (23). The PCR conditions are essentially as described elsewhere (23) and the products were electrophoresed on 1.2% agarose gels, visualized by ethidium bromide staining and compared with the intensity of co-amplified *18S* RNA.

Allele-specific transcription analysis. Allele-specific transcription was determined by comparing sequencing chromatographs of gene transcripts (cDNA) and matched genomic DNA. Potential SNPs mapping within the transcribed sequence of test genes were identified from the dbSNP database (ncbi.nlm.nih.gov). Coding SNPs were aligned to chromosome X according to the base pair position in the gene transcript, using the UCSC Genome Browser (May 2004, hg 17 Assembly; genome.ucsc.edu). Regions containing potential SNPs were amplified using primer sets designed with the Primer3 software (frodo.wi.mit.edu/cgi-bin/primer3/primer3_www.cgi). Genomic DNA and cDNA were PCR amplified, essentially as described above and sequenced at the Laboratoire d'Analyse et de Synthèse d'Acides Nucléiques (Université Laval, Quebec). Primer sets and PCR conditions are available at www.toninlab.mcgill.ca. Chromatographs were analyzed using Chromas© software by Technelysium (technelysium.com.au/chromas.html).

Allelotype analysis. A PCR-based assay was used to allelotype 24 polymorphic microsatellite repeat markers distributed along chromosome X as described previously (35). Primer sets for the markers *DXS1068, DSX1226, DXS7108, DXS7119, DXS7163, DXS8022, DXS8029, DXS8051, DXS8063, DXS8074, DXS991, DXS992, GATA160B08, AR*, and *HPRT* are available from The GDB Human Genome Database (www.gdb.org). In order to represent all major chromosome X cytobands and regions harboring genes of interest, nine additional markers (*MHBPNT1, MHBPNT2, MHBPNT3, MHBPNT4, MHBPNT5, MHBPNT6, MHBPNT7, MHBPNT8,* and *MHBPNT9*) were designed from simple repeat tracks reported in the UCSC Genome Browser (July 2003 hg 16 Assembly) (genome.ucsc.edu) using Primer3 software (frodo.wi.mit.edu/cgi-bin/primer3/primer3_www.cgi). The primer pairs for these genetic markers are available at www.toninlab.mcgill.ca. In the absence of reference normal matching genomic DNA for most of the EOC cell lines, alleles were only scored based on the intensity of the banding patterns from autoradiograms.

Barr body staining. Harvested cells from OV90, TOV21G, TOV81D and TOV112D were washed twice in 0.9% NaCl, fixed with 3:1 methanol/acetic acid (v:v) and dropped on glass slides. Slides were dipped into a 5 N HCl solution for 10 min, washed in distilled water for 20 min, stained for 15 min with 1% cresyl violet acetate (Sigma), washed in distilled water and air dried. Female and male oral mucosa cells, karyotyped for chromosome content, were used as positive and negative controls, respectively. Approximately 300 nuclei for each sample were scored for the presence of a Barr body using a Zeiss Imager.Z1 (Zeiss, Toronto, Ontario) with a bright field microscope equipped with a digital color camera MRC5 and AxioVision 4.3 capturing software. A 15% cut-off was used for Barr body positivity (36).

FISH analysis. Cells from OV90, TOV21G, TOV81D and TOV112D were treated with 0.02 μg/ml of colcemid (Invitrogen, Burlington, Ontario) for 3 h and harvested for metaphase chromosome preparations according to established procedures (37). FISH analysis with a chromosome X whole chromosome painting (WCP-X) probe (QBiogene, Illkirch, France) was carried out following the manufacturer's instructions. Hybridized metaphases were observed using an epifluorescence Zeiss Imager.Z1 microscpe equipped with a digital camera Axio Cam MRm and AxioVision 4.3 capturing software (Zeiss).

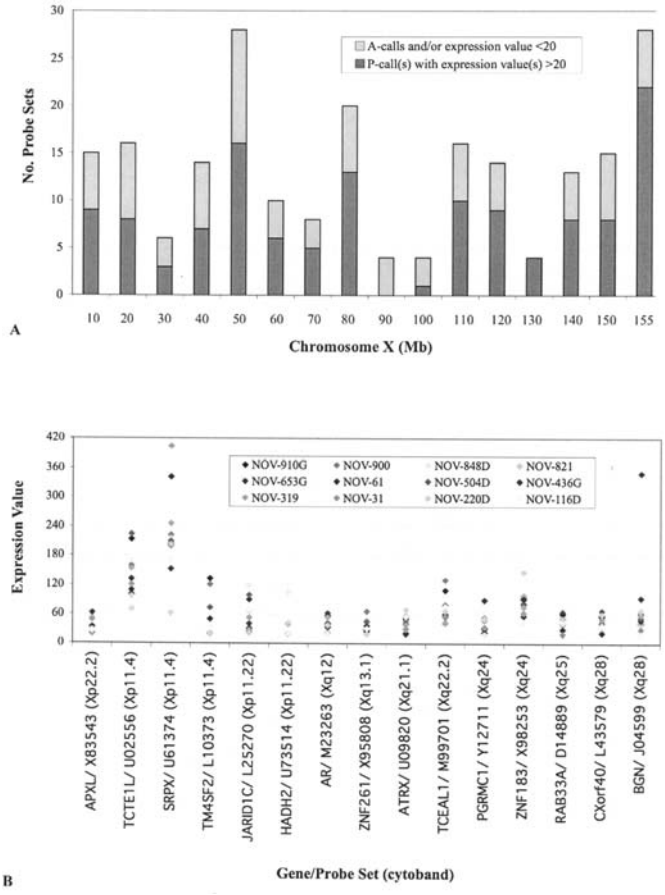

Figure 1. Microarray expression analysis of NOSE samples. A, the distribution of expression values (>20 or <20) along with their reliability scores (P call = high reliability score, and A call = low reliability score) relative to position of probe sets along chromosome X (organized from X*ptel* at 0 Mb to X*qtel* at 155 Mb). B, the expression values of primary cultures of NOSE samples for those probe sets exhibiting a >3-fold difference in the range of expression relative to the maximum and minimum values of expression observed in the set of 12 samples tested. The expression values are organized relative to cytoband position on chromosome X based on UCSC Human Genome Browser. Both the abbreviated gene name and probe set number are provided.

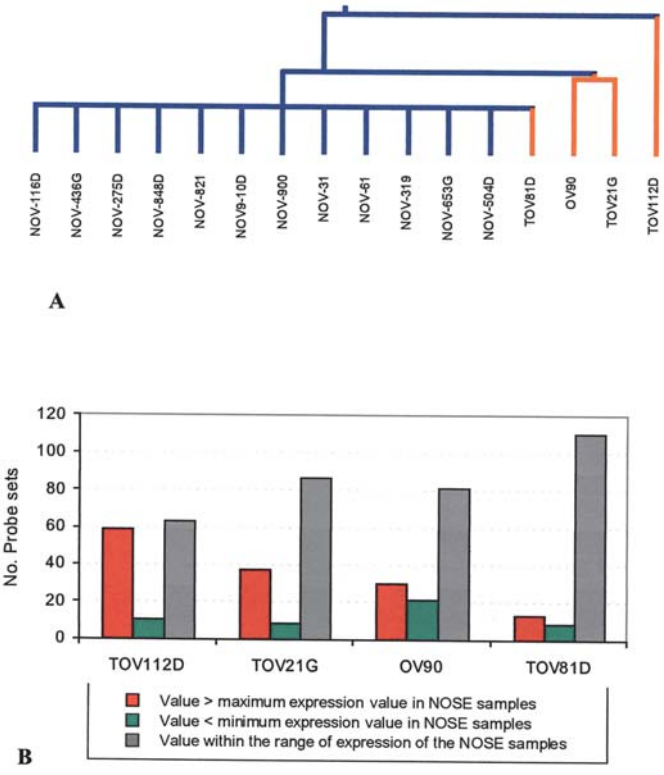

Figure 2. Global analysis of gene expression of the EOC cell lines and NOSE samples. A, hierarchical cluster analysis of primary cultures of NOSE samples (NOV samples) and four EOC cell lines, TOV81D, OV90, TOV21G and TOV112D. B, the proportion of probe sets exhibiting values of expression of each EOC cell line falling outside and within the range of expression of NOSE.

Results

Transcriptome analysis of the primary cultures of NOSE samples. The chromosome X transcriptome was derived from primary cultures of 12 NOSE samples using the Affymetrix GeneChip HuGeneFL array. This microarray contained 215 probe sets representing 195 genes or expressed sequences of the estimated 1141 genes located on chromosome X (NCBI Map Viewer, ncbi.nlm.nih.gov) (Fig. 1). Based on two-way comparative analyses the expression values were highly correlated (with correlation coefficients >95%). Approximately 27% (n=57) of the probe sets exhibited expression values <20 with a low reliability score (A calls). Approximately 56% (n=121) of the probe sets exhibited expression values >20 with a high reliability score (P calls) in at least one NOSE sample; and 22 of these probe sets (18%) varied at least 3-fold when the maximum and minimum values of expression were compared. An investigation of the target sequences of the probe sets using the NetAffx® Analysis Center in combination with sequence information from the UCSC Human Genome Browser revealed that seven of these 22 probe sets were not complementary to the transcript of the intended target gene. The expression values for the remaining 15 genes and their chromosomal positions are shown in Fig. 1. With the exception of *SRPX* and *BGN*, the range of expression of the majority of genes was <4-fold when the maximum and minimum expression values were compared. The genes exhibiting >3-fold differences in expression in the NOSE samples were not associated with a particular chromosomal region.

Comparative analysis of NOSE samples and the EOC cell lines. HuGeneFL array analysis was also performed on four well-characterized spontaneously immortalized EOC cell lines (TOV21G, TOV81D, TOV112D, and OV90) using the extracted data from 215 probe sets representing the chromosome X genes. The expression values of TOV21G, TOV81D, and OV90 were each highly correlated with the 12 NOSE samples in two-way comparative analyses of correlation coefficients of the expression data (range, 89%-99% similarity), in contrast to that of TOV112D (56-69%). When the EOC cell lines were compared to one another, the expression values were the least correlated in two-way comparisons with TOV112D (53-74%), in contrast to two-way comparative analyses of TOV21G, TOV81D, and OV90, where correlation coefficients varied from 87% to 90%. Hierarchical cluster analysis of NOSE samples and EOC cell lines, showed that TOV112D differed the most from all samples tested and TOV81D clustered with the NOSE samples (Fig. 2). Approximately

Table I. Differentially expressed genes identified by HuGeneFL microarray analysis

Probe	Gene			NOSE[d]			TOV81D[e]			OV90[e]			TOV21G[e]			TOVl12D[e]		
set	symbol	XCI[c]	Cytoband	MAX	MIN	F	V	C	F	V	C	F	V	C	F	V	C	F
M16279	*CD99*[a]	E	Xp22.33	945	517	2	938	P		621	P		356	P	-1	166	P	-3
M17733	*TMSB4X*[b]	E	Xp22.2	3818	2559	1	2816	P		4014	P	1	2367	P	-1	20	A	-128
Y07867	*PIR*[b]	E	Xp22.2	28	20	1	20	P		78	P	3	20	P		38	P	1
X72841	*RBBP7*[a]	E	Xp22.2	216	133	2	128	P	-1	250	P	1	446	P	2	223	P	1
U08316	*RPS6KA3*[b]	S	Xp22.12	26	20	1	60	P	2	149	P	6	90	P	3	34	P	1
L19161	*EIF2S3*	E	Xp22.11	23	20	1	27	P	1	133	P	6	483	P	21	79	P	3
U61374	*SRPX*[a]	S	Xpll.4	404	62	7	97	P		26	P	-2	20	P	3	57	P	-1
U50553	*DDX3X*[b]	E	Xpll.4	30	20	1	63	P	2	31	P	1	87	P	3	69	P	2
D86969	*PHF16*	S	Xpll.3	20	20	1	20	A		20	A		32	P	2	88	P	4
M25269	*ELK1*[b]	S	Xpll.23	22	20	1	27	P	1	31	P	1	20	P		91	P	4
Z37986	*EBP*[b]	S	Xpll.23	157	81	2	122	P		433	P	3	219	P	1	86	P	
U77735	*PIM2*[b]	S	Xpll.23	22	20	1	20	A		66	P	3	52	A	2	26	A	1
M69066	*MSN*[a]	S	Xql2	1059	729	1	1041	P		206	P	-4	480	P	-2	569	P	-1
D83783	*MED12*	S	Xql3.1	26	20	1	20	A		20	A		20	P		93	P	4
D00860	*PRPS1*[b]	S	Xq22.3	76	37	2	100	P	1	203	P	3	166	P	2	98	P	1
Y12711	*PGRMC 1*	S	Xq24	90	20	4	201	P	2	180	P	2	185	P	2	111	P	1
J02683	*SLC25A5*[b]	S	Xq24	398	229	2	320	P		1178	P	3	1050	P	3	934	P	2
M31642	*HPRT1*	S	Xq26.2	90	48	2	64	P		92	P	1	163	P	2	171	P	2
L43579	*CXorf40*[b]	S	Xq28	68	22	3	50	P		76	P	1	73	P	1	112	P	2
U47105	*NSDHL*	S	Xq28	68	32	2	62	P		72	P	1	96	P	1	68	P	

These genes have been independently studied in the context of [a]ovarian cancer or [b]cancers of other sites. [c]Subject to XCI (S) or escaping XCI (E) inferred from Carrel *et al* (38). [d]Maximum (MAX) and minimum (MIN) values of NOSE samples and fold difference (F) between MAX and MIN; and [e]expression value (V) and reliability score or call (C) of EOC cell lines, and fold differences (F) relative to the MIN (for values less than the NOSE MIN, negative value) or MAX (for values greater than the NOSE MAX, positive value) expression value of the NOSE samples.

29% (n=62) of the probe sets exhibited expression values <20 with poor reliability scores (A calls) in all EOC cell lines, where 42 of these probe sets also exhibited similar low values of expression and poor reliability scores in each of the 12 NOSE samples.

The expression values of probe sets for each of the EOC cell lines were compared to the maximum and minimum values of expression observed in the 12 NOSE samples. For this analysis only 134 (51 Xp arm probe sets and 83 Xq arm probe sets) of 215 probe sets were analyzed further as they exhibited expression values >20 and at least one high reliability score among the samples tested. In contrast to the tumorigenic EOC cell lines (TOV112D, TOV21G, and OV90), the non-tumorigenic EOC cell line (TOV81D) exhibited the smallest number of probe sets with expression values that fell outside the range of expression of the NOSE samples (Fig. 2). There were more probe sets exhibiting overexpression than underexpression in all EOC cell lines relative to the range of expression of the NOSE samples. OV90 exhibited a larger number of underexpressed probe sets that mapped to Xq (n=18, 13%) than to Xp (n=4, 3%), however this observation was not statistically significant (p>0.05) (Supplementary data available on request). TOV112D exhibited the largest number of probe sets (n=70, 52%) with values outside the range of expression of NOSE samples. Although there were more probe sets exhibiting overexpression on the Xq arm (n=39, 29%) than on the Xp arm (n=20, 15%) in this cell line, these observations were not statistically significant (p>0.47). The tumorigenic EOC cell lines had similar proportions of probe sets exhibiting values greater than the maximum expression of the NOSE samples for the Xp arm genes: 15% (n=20), 13% (n=17), and 13% (n=17) for TOV112D, TOV21G, and OV90, respectively. Both TOV112D and TOV21G exhibited the largest number of probe sets [n=59 (44%) and n=38 (28%), respectively] with values greater than the maximum value of expression observed in the NOSE samples (Fig. 2). These cell lines also exhibited the largest number of probe sets with values >1.5-fold and 2-fold relative to the maximum value of the NOSE samples (data not shown). Approximately 21% (n=28) of the probe sets exhibited expression values that fell outside the range of expression of the NOSE samples in all EOC cell lines or in all of the tumorigenic EOC cell lines (TOV21G, TOV112D, and OV90) and/or exhibited a minimum 3-fold difference in expression in at least one EOC

cell line in comparison to the maximum or minimum value of expression of the NOSE samples. Eight of these probe sets were not complementary to the target gene and thus were not investigated further. The expression patterns for the remaining 20 probe sets is shown in Table I. Noteworthy is that the majority of probe sets with expression values outside the range of expression of NOSE exhibited differences in expression <3-fold relative to the minimum or maximum value of expression of the 12 NOSE samples (data not shown), suggesting that small changes in overall gene expression occurred in the EOC cell lines.

XIST expression. *XIST* expression was investigated based on the rationale that the higher expression values of chromosome X genes in TOV112D relative to the NOSE samples could be due to alteration of XCI as a result of loss of *XIST* expression. *XIST* expression was not detectable by RT-PCR analysis of TOV112D and TOV21G in contrast to TOV81D and OV90, and the NOSE samples (Fig. 3). Comparable results were also obtained in PCR-based assays that incorporated radioactively labeled isotopes (data not shown). A series of malignant ovarian tumor samples were also investigated for *XIST* expression. As shown in Fig. 3, *XIST* expression was detectable by RT-PCR in the majority of EOC samples tested but was expressed at very low levels in four of 15 (27%) EOC samples, TOV921G, TOV1118D, TOV837, and TOV1054G. Although the assay is semi-quantitative, these EOC samples show abundant levels of *18S* RNA comparable to other EOC samples tested, suggesting that low detectable levels reflect low abundance of *XIST* transcripts.

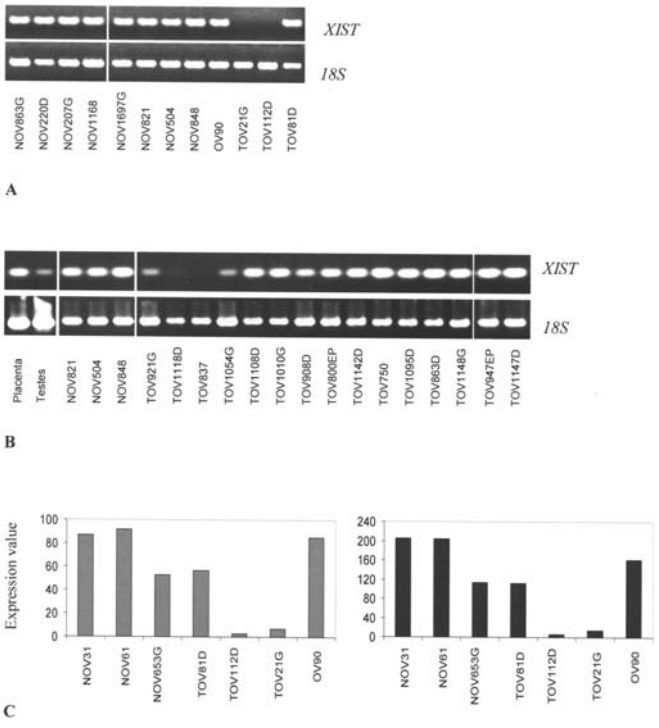

Figure 3. *XIST* expression analysis. A, RT-PCR results of *XIST* expression analysis of primary cultures of NOSE samples and the EOC cell lines including an *18S* control. B, RT-PCR analysis of malignant ovarian tumor (TOV) samples, primary cultures of NOSE samples, placenta and testes, including an *18S* control. C, microarray expression data of two different probes sets representing *XIST* from HG-133A array analysis of primary cultures of NOSE samples and the EOC cell lines.

Allele-specific transcription and allelotype of chromosome X in the EOC cell lines. Allele-specific gene expression in the EOC cell lines was investigated based on the rationale that the increased expression observed in TOV112D or TOV21G could be due to transcriptional reactivation of genes affected by XCI, as a result of loss of *XIST* expression. To expand the number of candidates for this investigation, the Affymetrix HG-133A array was used because of the higher density of probe set representing chromosome X genes relative to the HuGeneFL array. This microarray contained 766 probe sets representing 521 chromosome X genes. Given the overall similarity in gene expression profiles exhibited by HuGeneFL array analyses, only three NOSE samples were used in comparative analyses with the EOC cell lines. This is further shown by the expression values of 766 probe sets which were highly correlated (with correlation coefficients >88%) in two-way comparative analyses of the NOSE samples. Approximately 5% (n=36) of probes sets exhibited expression values that varied >3-fold when the maximum and minimum values of the NOSE samples were compared. Within this group were probe sets that represented genes such as *ATRX, BGN, FHL1, PGRMC1,* and *SRPX*, that varied >3-fold by both the HuGeneFL and HG-133A array analyses of the NOSE samples. Hierarchical cluster analysis of these 766 probe sets using data sets containing the NOSE and EOC cell lines was consistent with the results obtained in a comparable analysis of 215 chromosome X probe sets from the HuGeneFL array (data not shown). Unlike the HuGeneFL array, the HG-133A array contained two probe sets representing *XIST*. Noteworthy is that *XIST* expression by microarray analysis was comparable to results observed by RT-PCR analysis of the EOC cell lines (Fig. 3).

Genes with known XCI status based on a review of the literature [conducted prior to the recent publication of a study by Carrel *et al* (38)] were selected for further analysis based on those exhibiting a ≥2-fold expression value (P call) in TOV112D and/or TOV21G relative to the mean value of expression of the NOSE samples by HG-133A (n=62 genes) and HuGeneFL (n=35 genes) array analyses. Using these criteria, 71 genes were identified where 46 were known subjected to XCI, 18 were known to escape XCI and seven were known to exhibit heterogeneity of XCI. From this list, 17 genes were further investigated for allele-specific transcription in the EOC cell lines. An average of four coding single nucleotide polymorphisms (cSNPs) (range, 1-13 cSNPs investigated per gene) were identified for 15 of the 17 candidates based on publicly available data (Table II). As no cSNPs were reported for *HADH2A* and *PHKA1*, the 3'UTRs were sequenced in an attempt to identify novel polymorphisms. Sequence variations were not detected and, thus, these genes were not investigated further. Only four of the 17 genes investigated, *NONO, SLC25A5, DKC1*, and *FHL1*, were heterozygous in at least one of the EOC cell lines and all of these genes are known to be subjected to XCI. TOV81D was heterozygous for *NONO* and *SLC25A* and only one allele was expressed. OV90 was heterozygous for *DKCI* and only one allele was expressed. TOV21G was heterozygous for *NONO, SLC25A*, and *FHL1*.

Table II. Genes investigated for allele-specific transcription.

Gene symbol	Cytoband	XCI[a]	Probe set[b]	NOSE[c]	TOV81D[d]			OV90[d]			TOV21G[d]			TOV112D[d]			SNP (rs number)[e]
				Mean V	V	C	F	V	C	F	V	C	F	V	C	F	
MID1	Xp22.22	S	203637_s_at	18	20	P	1	59	P	3	262	P	15	164	P	9	1802190; 741500; 1802191
POLA	Xp22.11	S	204835_at	21	24	A	1	86	P	4	23	P	1	66	P	3	l1573534; 11573531; 11573532; 11573533; 6629934
RBM10	Xpll.3	S	D50912_at*	30	20	A		48	P	2	37	A	1	107	P	4	12008422; 5952419
			208984_x_at	73	56	P		104	P	1	80	P	1	237	P	3	
			215089_s_at	87	44	P		98	P	1	73	P		217	P	3	
			217221_x_at	51	35	P		68	P	1	47	P		143	P	3	
UBE1	Xpll.3	E	200964_at	823	745	P		642	P		1311	P	2	1375	P	2	1127319; 1804872; 22301147; 14952; 2228658
USP11	Xpll.3	H	208723_at	58	66	P	1	99	P	2	139	P	2	161	P	3	l319
SUV39H1	Xpll.23	S	218619_s_at	35	25	A		67	P	2	40	P	1	125	P	4	3373
PLP2	Xpll.23	S	I09604_at*	461	738	P	2	269	P		584	P	1	1281	P	3	1063508; 1063509; 1802970; 1802971; 1802968
			201136_at	209	519	P	2	68	P		136	P		378	P	2	
HADH2A	Xpll.22	S	U73514_at*	31	20	P		120	P	4	88	P	3	128	P	4	N/A
			202282_at	230	179	P		277	P	1	235	P	1	695	P	3	
KIF4A	Xql3.1	S	218355_at	32	26	P		133	P	4	56	P	2	372	P	12	1046485; 1046487; 1046488; 1046489; 1046490; 3186470; 3186472; 3752322
ZNF261	Xql3.1	S	X95808_s_at*	34	20	A		20	P		59	P	2	83	P	2	2272778; 1803003; 1803002; 3183972; 1803004; 1803001
			207559_s_at	36	36	P		49	P	1	74	P	2	100	P	3	
NONO	Xql3.1	S	U02493_at*	372	290	P		494	P	1	552	P	1	1690	P	5	1136472; 1802558; 2794; 3199958; 3208714; 1059295
			200057_s_at	571	758	P	1	880	P	2	648	P	1	1661	P	3	
			208698_s_at	115	217	P	2	374	P	3	127	P	1	394	P	3	
			210470_x_at	153	402	P	3	431	P	3	171	M	1	545	P	4	
PHKA1	Xql3.1	S	X73874_at*	20	20	A		20	P		20	M		42	P	2	N/A
			205450_at	25	34	P	1	34	P	1	45	P	2	73	P	3	
CSTF2	Xq22.1	S	204459_at	46	51	P	1	132	P	3	47	P	1	149	P	3	11553614; 7062004
TMSNB	Xq22.1	S	D82345_at*	23	20	A		20	P		137	P	6	64	P	3	1802647; 11557378
			205347_s_at	25	28	P	1	29	P	1	73	P	3	150	P	6	
SLC25A5	Xq24	S	J02683_s_at*	343	320	P		1178	P	3	1050	P	3	934	P	3	12390; 3147; 3146
FHL1	Xq26.3	S	U60115_at*	77	87	P	1	20	A		20	P		251	P	3	1802950; 1802951; 2746; 9018
			201539_s_at	21	39	P	2	15	P		15	A		43	P	2	
			201540_at	120	92	P		21	P		16	P		286	P	2	
			210298_x_at	21	33	A	2	15	A		15	A		43	P	2	
			210299_s_at	22	17	P		15	A		15	A		53	P	2	
			214505_s_at	30	34	P	1	15	A		15	A		54	P	2	
DKC1	Xq28	S	201478_s_at	105	82	P		271	P	3	154	P	1	389	P	4	2853347; 2728532; 5945234; 2728533; 2853350; 2853355; 3752356; 3752357; 1800533
			201479_at	223	177	P		391	P	2	279	P	1	713	P	3	7878787; 11795799; 2728534; 11795799

[a]XCI status, subjected to XCI (S), escaping XCI (E) and heterogenous XCI (H) based on Carrel *et al* (38); [b]Probe sets from HuFL dataset (*); [c]Mean NOSE expression value (V); [d]expression value (V), reliability score (C), and fold difference (F) relative to mean value of expression of NOSE samples (only fold differences greater than mean NOSE values are shown); [e]SNP number in dbSNP database (NCBI; http://www. ncbi.nlm.nih.gov/entrcz/query.fcgi?db=Snp).

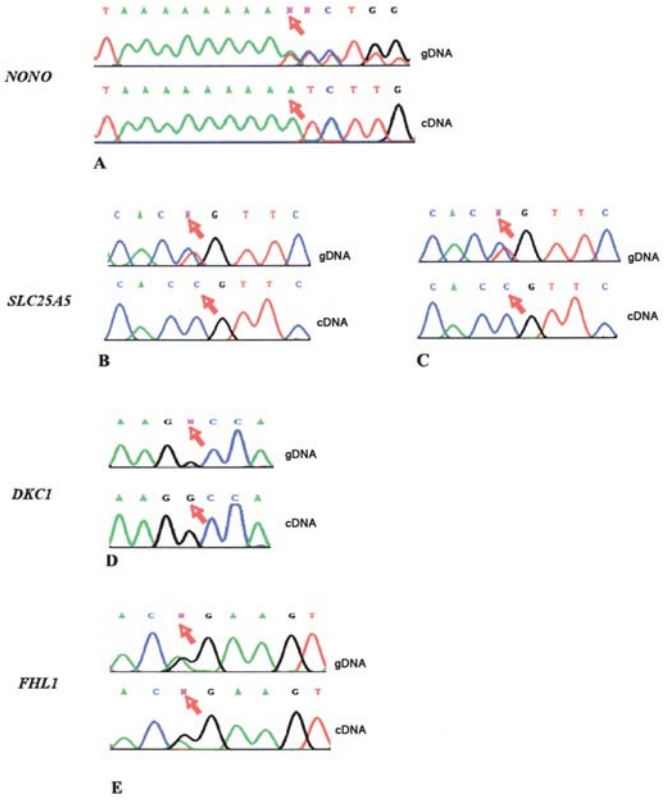

Figure 4. Allele specific expression of chromosome X genes in the EOC cell lines. Chromatograms are shown for cDNA and corresponding genomic DNA (gDNA) representing *NONO* for TOV21G (A), *SLC25A5* for TOV81D (B) and OV90 (C), *DKCI* for OV90 (D), and *FHL1* for TOV21G (E). The arrow indicates differences in allelic content of the sequence.

Cytoband	Position (bp)	Marker	HTZ	EOC Cell Lines			
				TOV112D	OV90	TOV21G	TOV81D
Xp22.2	9,308,966	*DXS8051*	0.87				
Xp22.2	10,001,962	*DXS7108*	0.75				
Xp22.2	13,694,363	*DXS8022*	0.81				
Xp22.22	14,459,111	*MHBPNT1*	-				
Xp22.13	18,814,202	*DXS7163*	0.76				
Xp22.11	22,707,079	*DXS1226*	0.85				
Xp22.11	24,641,592	*MHBPNT2*	-				
Xp21.2	30,409,960	*DXS992*	0.87				
Xp11.4	38,664,206	*DXS1068*	0.82				
Xp11.3	46,736,353	*GATA160B08*	-				
Xp11.23	48,749,105	*MHBPNT3*	-				
Xp11.21	55,402,060	*DXS991*	0.82				
Xq12	64,725,009	*DXS8029*	0.22				
Xq12	66,548,098	*AR*	0.90				
Xq13.1	70,237,162	*DXS7119*	-				
Xq13.2	72,795,535	*MHBPNT4*	-				
Xq21.1	77,165,871	*MHBPNT5*	-				
Xq22.1	100,576,455	*MHBPNT6*	-				
Xq22.1	101,004,404	*DXS8063*	0.83				
Xq24	118,381,533	*MHBPNT7*	-				
Xq26.2	133,334,735	*HPRT*	0.78				
Xq26.3	133,809,282	*DXS8074*	0.60				
Xq26.3	136,145,619	*MHBPNT8*	-				
Xq28	153,464,326	*MHBPNT9*	-				

Figure 5. Heterozygosity of chromosome X in EOC cell lines. Polymorphic microsatellite repeat markers were used to assess the heterozygosity of chromosome X in the EOC cell lines. The markers are available from the GDB Human Genome Database (www.gdb.org) and those given *MHBPNT* designations were designed from genomic sequence information available through the UCSC Human Genome Browser as described in the text. The data is organized relative to their cytoband and position on the X chromosome. The maximum heterozygosity (HTZ) indicated is from the GDB Human Genome Database; -, unknown HTZ. Loss of heterozygosity (dark grey), retention of heterozygosity (light grey), and no data (blank cell).

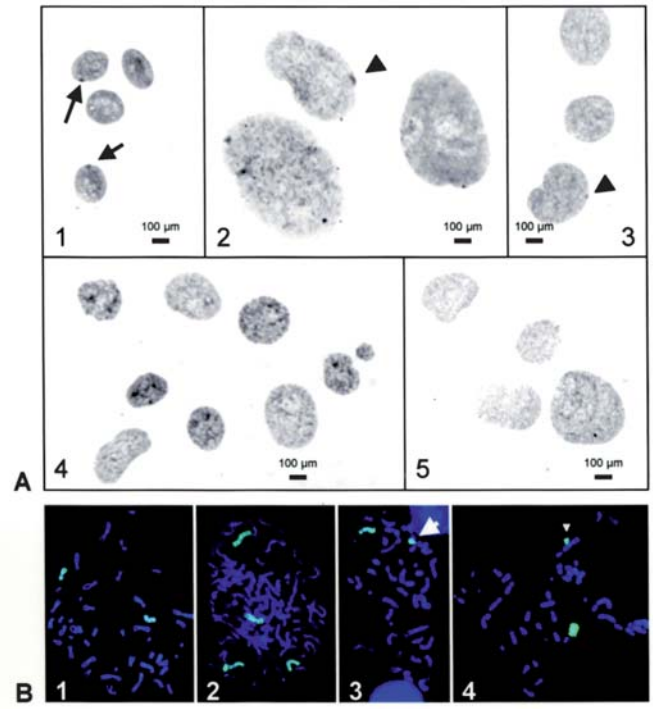

Figure 6. Barr body and cytogenetic analysis of chromosome X in the EOC cell lines. A, Barr body staining of oral mucosa cells from a normal human female (1), and the EOC cell lines TOV81D (2), OV90 (3), TOV21G (4) and TOV112D (5). The cells were fixed with cresyl violet solution. The arrows indicate Barr body chromatin staining. The arrowheads point to atypical (small) Barr body size. B, metaphase chromosomes of the EOC cell lines TOV81D (1), OV90 (2), TOV21G (3) and TOV112D (4), hybridized with an FITC-whole chromosome X painting probe. Whole-stained chromosome X is observed in metaphases of TOV81D (1) and OV90 (2) whereas a rearrangement of chromosome X and an autosome is observed in TOV21G (3, arrow) and truncated abnormal chromosome X is observed in TOV112D (4, arrowhead).

While only one *NONO* and *SLC25A* allele was expressed in TOV21G, the transcription of both *FHL1* alleles was detectable by sequence analysis of cDNA prepared from this EOC cell line. *FHL1* is known to be subjected to XCI and *a priori* transcription of only one allele is expected. Moreover, genomic sequence analysis of *NONO* in TOV21G revealed a mutation whereby an additional A was inserted in a poly-A repeat of the 3'UTR sequence of this gene corresponding to 2376insA based on reference sequence NM_007363. This result is not surprising given that TOV21G has been shown to exhibit microsatellite instability (24). Nevertheless, this sequence variant was not expressed based on sequence analysis of cDNA. Representative results are illustrated in Fig. 4. In contrast, none of the genes tested exhibited heterozygosity in TOV112D and thus it was not possible to assay for biallelic expression of the tested genes in this EOC cell line.

Given the paucity of polymorphic cSNPs in TOV112D, polymorphic microsatellite repeat markers were used to further assess heterozygosity of chromosome X. The genetic markers were selected from public databases or designed from sequence composition from the UCSC Human Genome Browser for genotyping analysis based on their location within or near the candidate genes of interest (Fig. 5). The heterozygosity status of the chromosome homologue was inferred as matching constitutional DNA from normal tissue was not

Table III. Barr body staining, XIST expression and chromosome X features of the EOC cell lines.

Cell line	Barr body analysis			*XIST* expression	Heterozygosity of chromosome X	Chromosome X status
	Cells with typical Barr body (%)	Cells with atypical Barr body (%)	Barr body status			
TOV81D	0	14	-	+	+	X,X
OV90	0	9	-	+	+	X,X,X,X
TOV21G	6	0	-	-	+	X, one X structural abnormality
TOV112D	2	0	-	-	-	X, one X structural abnormality
Female oral mucosa cells	20	0	+	ND	ND	XX
Male oral mucosa cells	1	0	-	ND	ND	XY

available for all of the EOC cell lines. Genotyping of TOV21G and OV90 suggested heterozygosity of a number of markers tested that represented different regions of both chromosome arms (Fig. 5). This is particularly evident for TOV21G where 20 of 24 (83%) markers tested exhibited heterozygosity. In contrast, all markers with the exception of that representing the androgen receptor locus (AR) were monoallelic in TOV112D. Sequence analysis revealed the presence of both alleles with one allele exhibiting a deletion of 33 nucleotides. The patient matched DNA from peripheral blood sample also exhibited heterogeneity of this locus. However, only one of the two alleles, the largest in both samples, was shared when tumor and constitutional DNA were compared. This was not observed with the other chromosome X polymorphic markers tested. This would imply that somatic mutation had occurred in the tumor sample from which the TOV112D cell line was derived. The allelic origin of the somatically derived variant cannot be determined. However, as this allele was the only example of heterozygosity it is possible that the mutation was derived from the chromosome X homolog retained after the occurrence of LOH and reduction to hemizygosity in TOV112D. The effect of the deletion, which occurred in the 5'UTR of AR, is not known. By Affymetrix GeneChip analysis AR expression was detectable at very low levels and numerous samples had low reliability scores (A calls) in NOSE samples (Fig. 1) and in all of the EOC samples (data not shown). Moreover, AR expression was not detectable by RT-PCR in any NOSE and EOC cell lines (data not shown).

*Barr body and FISH analysis of EOC cell line*s. The four EOC cell lines were tested for the presence of Barr bodies as loss of these structures and concomitant loss of *XIST* expression in cancer cell lines has been recently observed (39,40). None of the EOC cell lines exhibited typical Barr body staining (Table III). Less than 15% TOV21G and TOV112D nuclei stained positively for Barr bodies, and were therefore considered negative for the presence of an inactive chromosome X (36,41). Although Barr bodies were present in TOV81D and OV90, they were reduced in size in comparison to those observed in control female mucosa cells (Fig. 6). The presence of chromosome X was verified by metaphase FISH using a WCP-X probe (Fig. 6) (Table III). TOV81D and OV90 cell lines exhibited no apparent structural rearrangement of chromosome X consistent with previous G-banding results of these cell lines (24). Two normal copies of chromosome X were observed in TOV81D, and four copies in OV90. No other chromosome X derived cyotgenetic material was evident for TOV81D and OV90. In contrast TOV112D and TOV21G exhibited both a structurally normal chromosome X and rearrangements of chromosome X. In TOV21G, the abnormal chromosome X was the result of an unbalanced translocation with an autosome, as the WCP-X probe did not hybridize to the entire length of the derivative, and no extra WCP-X signal was observed on any other chromosome. The rearranged chromosome X in TOV112D only appeared to be the result of a deletion, as the derivative chromosome appeared smaller in size than a normal chromosome X and it completely hybridized with the WCP-X probe.

Discussion

Comparative analysis of chromosome X gene expression of four EOC cell lines with primary culture of 12 NOSE samples has identified differentially expressed genes as candidates for further study in ovarian tumorigenesis. Transcriptome analysis of the NOSE samples indicated a high degree of similarity in gene expression profiles. This was also suggested by the analysis of a smaller series of NOSE samples using the HG-133A, which contained a higher density of probe sets and more gene coverage of this chromosome. Not surprisingly, TOV81D exhibited the fewest differences in gene expression values when compared with the NOSE samples. This non-tumorigenic EOC cell line was derived from an ovarian cancer sample from a patient that exhibited the most indolent form of the disease (24). Similar findings were reported in microarray analyses using a prototype Affymetrix GeneChip that was used

for the investigation of global analysis of gene expression or chromosome 3 gene expression (19,20), and the HuGeneFL array analysis of chromosome 17 (21) and 22 (22) mapped genes. As has been observed in independent analyses of these EOC cell lines using earlier generation expression microarrays (19), and the analyses of genes located on chromosomes 3 (20), and 17 (21), there were more genes exhibiting overexpression than underexpression in all EOC cell lines relative to the range of expression of the NOSE samples. Hence, the overall modification of the chromosome X transcriptome is similar to that observed with other autosomes where there were more instances of overexpression relative to underexpression in the EOC cell lines than the NOSE samples.

At least three of the chromosome X genes, *SLC25A5*, *SRPX*, and *RBBP7*, which were differentially expressed in any of the EOC cell lines relative to NOSE samples, were also differentially expressed in a comparative HuGeneFL array analysis of low malignant potential ovarian tumors and malignant EOC samples (32). *SRPX* expression was also down-regulated in various cancers including lung (42), colorectal (43), and prostate (44) carcinomas. *SRPX* was shown to suppress anchorage-independent growth in *in vitro* assays using a number of human cancer cell lines including an ovarian cell line (45). In addition, *SRPX* maps within a minimal region of LOH in ovarian cancers (7,8). *RBBP7* has also been shown to interact with other known or suspected TSGs such as *RB1* (46) and *BRCA1* (47), and has been shown to suppress tumorigenicity and growth when induced in retinoblastoma (46) and breast cancer cell lines (48-50). Its role in the physiology and pathology of ovarian tissue was inferred in studies of transgenic mice with engineered disruptions in endocrine signaling showing differential expression of *RBBP7* (51). However, contrary to expectations based on these independent reports, *RBBP7* was overexpressed in the EOC cell lines relative to the NOSE samples in the present study as well as in malignant EOC samples relative to LMP samples in an independent study (32). As interpretation of expression microarray results may depend on the methods of analyses and samples used for comparative analyses (representative of different models of ovarian cancer), the significance of these findings warrants further investigation with validation of expression data at the transcriptional and protein level (52). Other differentially expressed genes identified in the present study have been implicated in ovarian cancer, such as *CD99* and *MSN*, or cancers of other sites, such as *TMSB4X, PIR, RPS6KA3, DDX3X, ELK1, EBP, PIM2, PRPS1, SLC25A5*, and *Cxorf40*. Moreover, although the EOC cell lines do not harbor *BRCA1* mutations (53), at least five differentially expressed genes, such as *EBP, MSN, CD99, EIF2S3*, and *ELK1* have been reported as overexpressed in *BRCA1*-linked ovarian cancers (54,55). These results suggest that the EOC cell lines and ovarian tumors exhibit dysregulation of common chromosome X genes.

The absence of *XIST* expression in TOV112D and TOV21G and possible effect of XCI status could account for the higher proportion of overexpressed genes relative to underexpressed genes observed in these EOC cell lines in comparison to OV90 and TOV81D. As expected for genes subjected to XCI, monoallelic expression was observed for *NONO* and *SLC25A5* in TOV21G and TOV81D, respectively, and for *DKCI* in OV90, although these EOC cell lines were heterozygous for these genes. In contrast, both alleles of *FHL1*, a gene subject to XCI were expressed in TOV21G. These results are consistent with alteration of XCI status in TOV21G. Heterozygous cSNPs were not found in genomic DNA for TOV112D and thus the allelic origin of gene transcription could not be discerned for genes such as *NONO, SLC25A5, DKCI*, and *FHL1*. In this cell line, it is possible that the majority if not all chromosome X loci were derived from the same parental homolog, as the heterozygosity of the *AR* locus could be explained by a somatic mutation derived from the chromosome X homolog retained after the occurrence of LOH and reduction to hemizygosity. In contrast, genotype analyses suggested the presence of both parental chromosome X homologs in TOV21G and OV90. Although this finding suggests that altered XCI status was associated with the loss of *XIST* expression, it is evident that reactivation of XCI genes was not applied globally in TOV21G as monoallelic expression of *NONO* was observed. This appears to be the case in murine cells, as previous studies have shown that loss of *Xist* expression destabilized XCI in somatic cells and increased the reactivation frequency of individual genes (56). A major challenge in the study of our EOC cell lines was the paucity of polymorphic chromosome X cSNPs available for biallelic expression analysis, an observation that perhaps is not surprising in light of recent evidence suggesting that the level of heterozygosity on the X chromosome is approximately 57% that of the autosomes (57). Although our findings need to be verified in a larger number of primary ovarian tumors and cell lines, they are consistent with two mechanisms that have been proposed to account for the absence of Xi in female cancers (58): Xi loss followed by Xa duplication to maintain diploid status and transcriptional reactivation of Xi (39,40), as proposed to have occurred in TOV112D and TOV21G, respectively.

The mechanisms underlying the absent *XIST* expression and the biological significance of Xi loss remain to be determined in ovarian cancer. Evidence suggesting that Xi loss could be common in female-specific cancers is based on the high frequencies of Barr body loss and absence of *XIST* expression (39,40). Consistent with these findings are our observations of the loss of the Barr body in TOV112D and TOV21G. Less than 15% of TOV112D and TOV21G nuclei exhibited a Barr body. Depending on the cell-type studied the threshold for Barr body positivity ranges from 15-35% for female oral mucosa cell scrapings and up to 90% for primary cultured female fibroblasts when most cells are in G2 (36,59,60). Based on FISH analysis of the EOC cell lines, both TOV112D and TOV21G also contained altered chromosome X suggesting that loss had occurred. TOV112D had an X chromosome of reduced size, and TOV21G exhibited an unbalanced X chromosome translocation. In OV90 and TOV81D, Barr body staining patterns were also atypical. We observed the presence of a small discrete region of perinuclear heterochromatic staining. Although certain variables are known to influence Barr body formation, size and number in non-cancerous cells, less is known about these influences in malignant ovarian cancer cells (36). Structural changes in the X chromosome may cause variations in the size of the Barr body because the abnormal X tends to be late-replicating (36). A more formal definition of positivity for Barr bodies requires that the staining should be considerably larger than that

observed in OV90 and TOV81D, suggesting that a deletion or partial reactivation of Xi could have occurred. However, both of these cell lines exhibited *XIST* expression and maintained genetic heterozygosity. Moreover FISH analysis did not reveal any cryptic rearrangement or gross deletions involving chromosome X material for TOV81D and OV90. Hence, the reduced amount of facultative heterochromatin staining is unlikely to be due to a major deletion or partial reactivation of the Xi chromosome.

Our analysis of a small series of malignant ovarian tumors demonstrated the absence of *XIST* expression in a subset of these tumors, suggesting that alteration of expression is not an artifact of cell culture. Indeed, the *XIST* expression profile of TOV112D, OV90, and TOV21G was not affected by cell growth conditions in that *XIST* expression was also not detectable by microarray analysis of TOV112D and TOV21G grown in cell culture as three-dimensional spheroids, or as tumor masses in *nude* mouse assays at either subcutaneous or intraperitoneal injection sites (unpublished data). Expression profiling studies have also implicated *XIST* expression in the clinical management of ovarian cancer patients since absent *XIST* expression has been shown to be associated with Taxol® resistance in ovarian tumors (61). Notable is that our recent analysis of the EOC cell lines showed no statistically significant difference in sensitivity to paclitaxel (Taxol) (53).

During the course of this investigation a more comprehensive list of genes subjected to XCI was published (38). We reviewed this list in relation to the expression pattern of the genes by HG-133A microarray analysis in the four EOC cell lines (Supplementary data available on request). There appears to be no overt pattern of expression that would suggest an alteration in gene expression that could be attributable to an alteration of XCI status. Moreover, there appeared to be no overt differences in overexpression of Xp genes as suggested by the analyses of earlier generation HuGeneFL GeneChip analyses as 44%-48% of overexpressed genes where located on the Xp arm in the tumorigenic EOC cell lines and 38% of overexpressed genes were located on the Xp arm in TOV81D. It is possible however, that changes in chromosome copy number due to aneuploidy and chromosomal rearrangement could influence the interpretation of these results. As suggested by the biallelic expression analysis of TOV21G, alteration of global XCI status may not be universally applied. Moreover, epigenetic modification of gene expression due to alteration in molecular pathways important in cancer is reflected in the global analysis of gene expression of the EOC cell lines, particularly in relation to the aggressivity of the cancer from which these cell lines were derived. The molecular characterization of overexpressed genes would be required to determine if perturbation of XCI is an epiphenomenon due to acquired cytogenetic abnormalities of female cancers or if there is a selective advantage conferred by overexpressed genes associated with Xa gain or Xi reactivation. Microarray analyses revealed differences in chromosome X gene expression in four EOC cell lines with distinct genetic backgrounds and biological phenotypes, irrespective of XCI status suggesting the importance of X-linked genes in ovarian cancer. Despite apparent differences in *XIST* expression, Barr body staining, chromosome X content, and the heterogeneity of chromosome X, there appeared to be modest differences in the chromosome X transcriptome in the EOC cell lines relative to the NOSE samples, suggesting that substantial feedback regulation may occur. However, based on the comparative analysis of EOC cell lines and NOSE samples, *XIST* expression and chromosome X content have revealed candidates both overexpressed and underexpressed relative to NOSE samples that could be explored further for their role in ovarian tumorigenesis.

Acknowledgements

We thank Lise Portelance, and Manon de Ladurantaye for their assistance, and Maisa Yoshimoto for her helpful expertise. M.-H. Benoît is a recipient of a graduate scholarship from the National Science and Engineering Research Council of Canada; T.J. Hudson is a recipient of an Investigator Award from the Canadian Institutes of Health Research (CIHR) and a Clinician-scientist Award in Translational Research from the Burroughs Welcome Fund. G. Maire is a recipient of the Helena H. Lam award. D. Provencher is a recipient of a Chercheur-Clinicien Senior, and A.-M. Mes-Masson is a recipient of a Chercheur National, all fellowships provided by the Fonds de la recherche en santé du Québec (FRSQ). J.A. Squire and G. Maire thank the Ontario Cancer Research Network for financial support. The ovarian tumor bank was supported by the Banque de tissus et de données of the Réseau de recherche sur le cancer of the FRSQ. This work was supported by a grant from the CIHR to A.-M. Mes-Masson, P.N. Tonin, D. Provencher and T.J Hudson.

References

1. Buekers TE, Lallas TA and Buller RE: Xp22.2-3 loss of heterozygosity is associated with germline BRCA1 mutation in ovarian cancer. Gynecol Oncol 76: 418-422, 2000.
2. Cheng PC, Gosewehr JA, Kim TM, *et al*: Potential role of the inactivated X chromosome in ovarian epithelial tumor development. J Natl Cancer Inst 88: 510-518, 1996.
3. Choi C, Cho S, Horikawa I, *et al*: Loss of heterozygosity at chromosome segment Xq25-26.1 in advanced human ovarian carcinomas. Genes Chromosomes Cancer 20: 234-242, 1997.
4. Edelson MI, Lau CC, Colitti CV, Welch WR, Bell DA, Berkowitz RS and Mok SC: A one centimorgan deletion unit on chromosome Xq12 is commonly lost in borderline and invasive epithelial ovarian tumors. Oncogene 16: 197-202, 1998.
5. Osborne RJ and Leech V: Polymerase chain reaction allelotyping of human ovarian cancer. Br J Cancer 69: 429-438, 1994.
6. Nakayama K, Takebayashi Y, Hata K, Fujiwaki R, Iida K, Fukumoto M and Miyazaki K: Allelic loss at 19q12 and Xq11-12 predict an adverse clinical outcome in patients with mucinous ovarian tumours of low malignant potential. Br J Cancer 90: 1204-1210, 2004.
7. Yang-Feng TL, Li S, Han H and Schwartz PE: Frequent loss of heterozygosity on chromosomes Xp and 13q in human ovarian cancer. Int J Cancer 52: 575-580, 1992.
8. Yang-Feng TL, Han H, Chen KC, *et al*: Allelic loss in ovarian cancer. Int J Cancer 54: 546-551, 1993.
9. Hogdall EV, Ryan A, Kjaer SK, *et al*: Loss of heterozygosity on the X chromosome is an independent prognostic factor in ovarian carcinoma: from the Danish 'MALOVA' Ovarian Carcinoma Study. Cancer 100: 2387-2395, 2004.
10. Arnold N, Hagele L, Walz L, Schempp W, Pfisterer J, Bauknecht T and Kiechle M: Overrepresentation of 3q and 8q material and loss of 18q material are recurrent findings in advanced human ovarian cancer. Genes Chromosomes Cancer 16: 46-54, 1996.
11. Diebold J, Deisenhofer I, Baretton GB, *et al*: Interphase cytogenetic analysis of serous ovarian tumors of low malignant potential: comparison with serous cystadenomas and invasive serous carcinomas. Lab Invest 75: 473-485, 1996.

12. Iwabuchi H, Sakamoto M, Sakunaga H, *et al*: Genetic analysis of benign, low-grade, and high-grade ovarian tumors. Cancer Res 55: 6172-6180, 1995.
13. Tibiletti MG, Bernasconi B, Taborelli M, *et al*: Genetic and cytogenetic observations among different types of ovarian tumors are compatible with a progression model underlying ovarian tumorigenesis. Cancer Genet Cytogenet 146: 145-153, 2003.
14. Wasenius VM, Jekunen A, Monni O, Joensuu H, Aebi S, Howell SB and Knuutila S: Comparative genomic hybridization analysis of chromosomal changes occurring during development of acquired resistance to cisplatin in human ovarian carcinoma cells. Genes Chromosomes Cancer 18: 286-291, 1997.
15. Brown CJ: Role of the X chromosome in cancer. J Natl Cancer Inst 88: 480-482, 1996.
16. Brown CJ, Carrel L and Willard HF: Expression of genes from the human active and inactive X chromosomes. Am J Hum Genet 60: 1333-1343, 1997.
17. Liao DJ, Du QQ, Yu BW, Grignon D and Sarkar FH: Novel perspective: focusing on the X chromosome in reproductive cancers. Cancer Invest 21: 641-658, 2003.
18. Spatz A, Borg C and Feunteun J: X-chromosome genetics and human cancer. Nat Rev Cancer 4: 617-629, 2004.
19. Tonin PN, Hudson TJ, Rodier F, *et al*: Microarray analysis of gene expression mirrors the biology of an ovarian cancer model. Oncogene 20: 6617-6626, 2001.
20. Manderson EN, Mes-Masson AM, Novak J, Lee PD, Provencher D, Hudson TJ and Tonin PN: Expression profiles of 290 ESTs mapped to chromosome 3 in human epithelial ovarian cancer cell lines using DNA expression oligonucleotide microarrays. Genome Res 12: 112-121, 2002.
21. Presneau N, Mes-Masson AM, Ge B, Provencher D, Hudson TJ and Tonin PN: Patterns of expression of chromosome 17 genes in primary cultures of normal ovarian surface epithelia and epithelial ovarian cancer cell lines. Oncogene 22: 1568-1579, 2003.
22. Arcand SL, Mes-Masson AM, Provencher D, Hudson TJ and Tonin PN: Gene expression microarray analysis and genome databases facilitate the characterization of a chromosome 22 derived homogeneously staining region. Mol Carcinog 41: 17-38, 2004.
23. Presneau N, Dewar K, Forgetta V, Provencher D, Mes-Masson AM and Tonin PN: Loss of heterozygosity and transcriptome analyses of a 1.2 Mb candidate ovarian cancer tumor suppressor locus region at 17q25.1-q25.2. Mol Carcinog 43: 141-154, 2005.
24. Provencher DM, Lounis H, Champoux L, *et al*: Characterization of four novel epithelial ovarian cancer cell lines. In Vitro Cell Dev Biol Anim 36: 357-361, 2000.
25. Jacobs IJ, Kohler MF, Wiseman RW, *et al*: Clonal origin of epithelial ovarian carcinoma: analysis by loss of heterozygosity, p53 mutation, and X-chromosome inactivation. J Natl Cancer Inst 84: 1793-1798, 1992.
26. Li S, Han H, Resnik E, Carcangiu ML, Schwartz PE, Yang-Feng TL: Advanced ovarian carcinoma: molecular evidence of unifocal origin. Gynecol Oncol 51: 21-25, 1993.
27. Abeln EC, Kuipers-Dijkshoorn NJ, Berns EM, Henzen-Logmans SC, Fleuren GJ and Cornelisse CJ: Molecular genetic evidence for unifocal origin of advanced epithelial ovarian cancer and for minor clonal divergence. Br J Cancer 72: 1330-1336, 1995.
28. Park TW, Felix JC and Wright TC Jr: X chromosome inactivation and microsatellite instability in early and advanced bilateral ovarian carcinomas. Cancer Res 55: 4793-4796, 1995.
29. Kupryjanczyk J, Thor AD, Beauchamp R, Poremba C, Scully RE and Yandell DW: Ovarian, peritoneal, and endometrial serous carcinoma: clonal origin of multifocal disease. Mod Pathol 9: 166-173, 1996.
30. Kruk PA, Maines-Bandiera SL and Auersperg N: A simplified method to culture human ovarian surface epithelium. Lab Invest 63: 132-136, 1990.
31. Lounis H, Provencher D, Godbout C, Fink D, Milot MJ and Mes-Masson AM: Primary cultures of normal and tumoral human ovarian epithelium: a powerful tool for basic molecular studies. Exp Cell Res 215: 303-309, 1994.
32. Ouellet V, Provencher DM, Maugard CM, *et al*: Discrimination between serous low malignant potential and invasive epithelial ovarian tumors using molecular profiling. Oncogene 24: 4672-4687, 2005.
33. Novak JP, Sladek R and Hudson TJ: Characterization of variability in large-scale gene expression data: implications for study design. Genomics 79: 104-113, 2002.
34. Ganesan S, Silver DP, Greenberg RA, *et al*: BRCA1 supports XIST RNA concentration on the inactive X chromosome. Cell 111: 393-405, 2002.
35. Dion F, Mes-Masson AM, Seymour RJ, Provencher D and Tonin PN: Allelotyping defines minimal imbalance at chromosomal region 17q25 in non-serous epithelial ovarian cancers. Oncogene 19: 1466-1472, 2000.
36. Barch M: The ATC Cytogenetics Laboratory Manual. Raven Press, New York, 1991.
37. Limon J, Dal Cin P and Sandberg AA: Application of long-term collagenase disaggregation for the cytogenetic analysis of human solid tumors. Cancer Genet Cytogenet 23: 305-313, 1986.
38. Carrel L and Willard HF: X-inactivation profile reveals extensive variability in X-linked gene expression in females. Nature 434: 400-404, 2005.
39. Kawakami T, Zhang C, Taniguchi T, *et al*: Characterization of loss-of-inactive X in Klinefelter syndrome and female-derived cancer cells. Oncogene 23: 6163-6169, 2004.
40. Sirchia SM, Ramoscelli L, Grati FR, *et al*: Loss of the inactive X chromosome and replication of the active X in BRCA1-defective and wild-type breast cancer cells. Cancer Res 65: 2139-2146, 2005.
41. Therman E: Human Chromosomes - Structure, Behavior, Effects. Springer-Verlag, New York, 1986.
42. Shimakage M, Takami K, Kodama K, Mano M, Yutsudo M and Inoue H: Expression of drs mRNA in human lung adenocarcinomas. Hum Pathol 33: 615-619, 2002.
43. Mukaisho K, Suo M, Shimakage M, Kushima R, Inoue H and Hattori T: Down-regulation of drs mRNA in colorectal neoplasms. Jpn J Cancer Res 93: 888-893, 2002.
44. Kim CJ, Shimakage M, Kushima R, Mukaisho K, Shinka T, Okada Y and Inoue H: Down-regulation of drs mRNA in human prostate carcinomas. Hum Pathol 34: 654-657, 2003.
45. Yamashita A, Hakura A and Inoue H: Suppression of anchorage-independent growth of human cancer cell lines by the drs gene. Oncogene 18: 4777-4787, 1999.
46. Guan LS, Rauchman M and Wang ZY: Induction of Rb-associated protein (RbAp46) by Wilms' tumor suppressor WT1 mediates growth inhibition. J Biol Chem 273: 27047-27050, 1998.
47. Yarden RI and Brody LC: BRCA1 interacts with components of the histone deacetylase complex. Proc Natl Acad Sci USA 96: 4983-4988, 1999.
48. Li GC, Guan LS and Wang ZY: Overexpression of RbAp46 facilitates stress-induced apoptosis and suppresses tumorigenicity of neoplastigenic breast epithelial cells. Int J Cancer 105: 762-768, 2003.
49. Zhang TF, Yu SQ, Loggie BW and Wang ZY: Inducible expression of RbAp46 activates c-Jun NH2-terminal kinase-dependent apoptosis and suppresses progressive growth of tumor xenografts in nude mice. Anticancer Res 23: 4621-4627, 2003.
50. Zhang TF, Yu SQ, Deuel TF and Wang ZY: Constitutive expression of Rb associated protein 46 (RbAp46) reverts transformed phenotypes of breast cancer cells. Anticancer Res 23: 3735-3740, 2003.
51. Burns KH, Owens GE, Ogbonna SC, Nilson JH and Matzuk MM: Expression profiling analyses of gonadotropin responses and tumor development in the absence of inhibins. Endocrinology 144: 4492-4507, 2003.
52. Le Page C, Provencher D, Maugard CM, Ouellet V and Mes-Masson AM: Signature of a silent killer: expression profiling in epithelial ovarian cancer. Expert Rev Mol Diagn 4: 157-167, 2004.
53. Samouelian V, Maugard CM, Jolicoeur M, *et al*: Chemosensitivity and radiosensitivity profiles of four new human epithelial ovarian cancer cell lines exhibiting genetic alterations in BRCA2, TGFbeta-RII, KRAS2, TP53 and/or CDNK2A. Cancer Chemother Pharmacol 54: 497-504, 2004.
54. Jazaeri AA, Yee CJ, Sotiriou C, Brantley KR, Boyd J and Liu ET: Gene expression profiles of BRCA1-linked, BRCA2-linked, and sporadic ovarian cancers. J Natl Cancer Inst 94: 990-1000, 2002.
55. Jazaeri AA, Chandramouli GV, Aprelikova O, *et al*: BRCA1-mediated repression of select X chromosome genes. J Transl Med 2: 32, 2004.
56. Csankovszki G, Nagy A and Jaenisch R: Synergism of Xist RNA, DNA methylation, and histone hypoacetylation in maintaining X chromosome inactivation. J Cell Biol 153: 773-784, 2001.

57. Ross MT, Grafham DV, Coffey AJ, *et al*: The DNA sequence of the human X chromosome. Nature 434: 325-337, 2005.
58. Dutrillaux B, Muleris M and Seureau MG: Imbalance of sex chromosomes, with gain of early-replicating X, in human solid tumors. Int J Cancer 38: 475-479, 1986.
59. Jolly C, Morimoto R, Robert-Nicoud M and Vourc'h C: HSF1 transcription factor concentrates in nuclear foci during heat shock: relationship with transcription sites. J Cell Sci 110: 2935-2941, 1997.
60. Puck TT and Johnson R: DNA exposure and condensation in the X and 21 chromosomes. Stem Cells 14: 548-557, 1996.
61. Huang KC, Rao PH, Lau CC, *et al*: Relationship of XIST expression and responses of ovarian cancer to chemotherapy. Mol Cancer Ther 1: 769-776, 2002.